Guided Ion Beam Studies of the Reactions of Fe^+ and Co^+ with CS_2 and COS

Chad Rue‡ and P. B. Armentrout*

Department of Chemistry, University of Utah, Salt Lake City, Utah 84112

Ilona Kretzschmar,† Detlef Schröder, and Helmut Schwarz*

Institut für Chemie der Technischen Universität Berlin, Strasse des 17. Juni 135, D-10623 Berlin, Germany

Received: May 31, 2001; In Final Form: July 16, 2001

The reactions of Fe^+ and Co^+ with CS_2 and COS are studied using guided-ion beam mass spectrometry. Dominant products in all four systems are MS^+ and MCX^+ (X = S, O). Cross sections for forming $FeCS^+$ and $CoCS^+$ in the CS_2 systems exhibit two endothermic features, which are assigned to the formation of different structural isomers. From the thresholds associated with forming CoS^+ and $CoCS^+$, we determine $D_0(Co^+-S) = 2.95 \pm 0.09$ eV and $D_0(Co^+-CS) = 2.68 \pm 0.34$ eV. These values are compared with $D_0(Fe^+-S) = 3.08 \pm 0.04$ eV and $D_0(Fe^+-CS) = 2.40 \pm 0.12$ eV determined previously, and the differences are discussed in some detail. The results for both metal ions reacting with CXS (X = S, O) suggest that the initial step is predominantly insertion of the metal ion into the C−S bond, with activation of the stronger C−O bond being less likely. Comparison of the energy-dependent cross sections indicates that both the CS_2 and COS systems show kinetic restrictions for Fe^+, which do not occur with Co^+. This difference can be attributed to changes of spin multiplicities in the various reactions, processes that are discussed in detail.

Introduction

Transition-metal sulfides are important components of various biological and industrial chemical processes. Vanadium, iron, nickel, copper, zinc, molybdenum, and tungsten are known to have sulfur coordination in many of the biological systems where they appear.[1−6] In industrial applications, transition-metal sulfides are used in a wide range of disciplines, including lubrication, energy storage, and catalysis.[1] For instance, a supported molybdenum/cobalt catalyst (where cobalt is believed to be the active site) is the most commonly used catalyst for hydrodesulfurization.[7] However, fundamental studies of the basic properties of transition metal sulfides, such as bond energies, have been slow to develop.

The present work is part of an ongoing collaborative project to systematically examine the reactions of transition-metal ions with the sulfur-transfer reagents CS_2 and COS. A particular interest in this work is to provide an accurate compilation of metal-sulfide bond energies. Previous work[8] has established the thermochemistry of scandium,[9] titanium,[9] vanadium,[10,11] chromium,[12] manganese,[12] and iron[13] sulfide cations. In these studies, we have observed reaction cross sections having unusual kinetic-energy dependences, which we attributed to competitive spin-allowed and spin-forbidden pathways in product formation. Such electronic-state effects, which appear to be common in transition-metal sulfur systems,[8,14] may be partially responsible for their chemical utility and versatility. In our previous work with iron,[13] results for guided ion beam results were reported for reaction of Fe^+ with CS_2, but the emphasis was strictly on the threshold behavior to determine the Fe^+-S and Fe^+-CS bond energies. Also ion cyclotron resonance (ICR) mass spectrometry results for the $Fe^+ + COS$ reaction were reported and used to refine the thermochemistry for FeS^+, but no guided ion beam results on this system were included. The thermochemical results from previous work[13] are included in Table 1 along with complementary literature thermochemistry. Here, we extend these studies to the reactions of cobalt cations and examine the iron systems in more detail. Co^+-S and Co^+-CS bond energies are derived and carefully compared to the corresponding data for iron. Further, the mechanisms for these reactions are explored in some detail. Related literature studies include IR spectroscopy on matrix isolated $Co^+(CS_2)$ and associated theoretical calculations.[15]

TABLE 1: Bond Dissociation Energies at 0 K

species	D_0 (eV)	species	D_0 (eV)
CO	11.109 (0.005)[a]	CS	7.37 (0.04)[b]
SC−O	6.88 (0.04)[c]	OC−S	3.140 (0.005)[c]
		CS_2	4.50 (0.04)[b,c]
FeO^+	3.47 (0.06)[d]	FeS^+	3.08 (0.04)[e]
CoO^+	3.25 (0.05)[d]	CoS^+	2.95 (0.09)[f]
FeC^+	4.08 (0.30)[g]	CoC^+	3.60 (0.30)[h]
Fe^+-CO	1.36 (0.08)[i]	Fe^+-CS	2.40 (0.12)[e]
Co^+-CO	1.80 (0.07)[j]	Co^+-CS	2.68 (0.34)[f]

[a] *NIST-JANAF Thermochemical Tables, Fourth Edition*; Chase, M. W. Ed.; J. Phys. Chem. Ref. Data, Monograph No. 9; American Chemical Society; 1998. [b] Prinslow, D. A.; Armentrout, P. B. *J. Chem. Phys.* **1991**, *94*, 3563. [c] Pedley, J. B.; Naylor, R. D.; Kirby, S. P. *Thermochemical Data of Organic Compounds*; Chapman and Hall: London, 1986. Corrected to 0 K using H° − H° (298.15) values taken from the reference in footnote *a*. [d] refs 34, 39, and 40. [e] ref 13. [f] This work. [g] ref 31. [h] ref 32. [i] refs 45 and 46. [j] ref 47.

Experimental Section

Guided Ion Beam Mass Spectrometer. The experiments were performed with a guided-ion beam mass spectrometer (GIBMS), which has been described in detail previously.[16,17] Briefly, M^+ (M = Fe, Co) ions are formed in a dc discharge

† Present address: Dept. Chem. & Chem. Biol., Harvard U., 12 Oxford St., Cambridge, MA 02138.

‡ Present address: IBM, P.O. Box 218, Yorktown Heights, NY 10598.

10.1021/jp0120716 CCC: $20.00
Published on Web 08/28/2001

flow tube (DC/FT) source, in which energetic Ar^+ ions sputter M^+ ions from a negatively charged (−1.5 to −2 kV) cathode comprising the metal to be studied. The ions formed in the source are then swept through a meter-long flow tube containing a 10% argon in helium buffer gas, at a total pressure of 0.7−1 Torr. The ions undergo ~10^5 collisions with the buffer gas as they traverse the flow tube, which helps to cool the ions to room temperature. However, it has been shown that helium is not always effective at quenching the excited electronic states of transition-metal ions.[8−10,13,18−20] Therefore, small amounts (40 mTorr or less) of methane cooling gas are added to the flow tube. Previous studies have demonstrated that methane quenches the electronic states of Fe^+ and Co^+ such that average electronic energies of the reactant ions are less than 0.03 eV.[19,20] No explicit contribution of such electronic excitation is included in the analyses below, but the final threshold values cited include this energy as part of their uncertainties.

Ions produced in the source are accelerated and passed through a magnetic sector for mass selection. The mass-selected ion beam is then focused into the entrance of a radio frequency (rf) octopole ion guide,[21] whose dc potential with respect to the ion source determines the kinetic energy of the ion beam. The rf potential on the octopole rods radially confines the ions and guides them through a gas cell, where a neutral reactant is introduced at pressures low enough (0.05−0.2 mTorr) to ensure single collision conditions. Both product and unreacted primary ions are extracted from the octopole and passed through a quadrupole for mass analysis. Finally, ions are detected with a secondary-electron scintillation ion detector and counted using standard pulse-counting techniques. This process is repeated at different collision energies simply by adjusting the dc octopole potential with respect to the ion source. Conversion of the raw ion intensities into cross sections and the calibration of the absolute energy scale are treated as described previously.[16] The accuracy of the product cross-section magnitudes is estimated to be ± 20%, and the uncertainty in the absolute energy scale is ± 0.05 eV (lab). Laboratory energies are converted to energies in the center-of-mass frame using $E_{CM} = E_{lab} \times M/(M + m)$, where M and m are the masses of the neutral and ionic reactants, respectively. This procedure accounts for conserving the momentum of the center-of-mass of the collision pair through the laboratory. Consequently, some of the laboratory energy is not available to the system to induce chemical change.

Energy thresholds for product formation at zero Kelvin, E_0, are obtained by modeling the cross sections using eq 1

$$\sigma(E) = \sigma_0 \Sigma g_i (E + E_i - E_0)^n/E^m \quad (1)$$

where σ_0 is an energy-independent scaling factor, and E is the relative kinetic energy. E_0, n, and m are treated as adjustable fitting parameters. The summation is over the rovibrational states of the neutral reactant having energies E_i and populations g_i ($\Sigma g_i = 1$). Before comparison to the data, eq 1 is convoluted over the kinetic energy distributions of both reactants. Because the convoluted form of eq 1 explicitly accounts for all of the energy available to the reaction, the optimized value of E_0 is interpreted as the threshold energy at zero Kelvin. Uncertainties in the values of E_0 obtained using eq 1 are derived from the range of fitting parameters that yield acceptable fits coupled with the uncertainties in the absolute energy scale and electronic energies of the reactant ions.

The parameter m is typically held at unity;[22,23] however, a value of $m = 1.5$ may be appropriate for spin-forbidden processes.[10] In the present work, some of the reactions are spin-forbidden, as discussed below. However, we have found previously in Cr^+/CS_2 and Mn^+/CS_2 reaction systems[12] that the choice of m need not have a large effect on the threshold energy, primarily because the adjustable parameter n compensates for variations in m. Our analysis of the present data yields a similar conclusion. Hence, we report only analyses for $m = 1$ and increase the uncertainty accordingly.

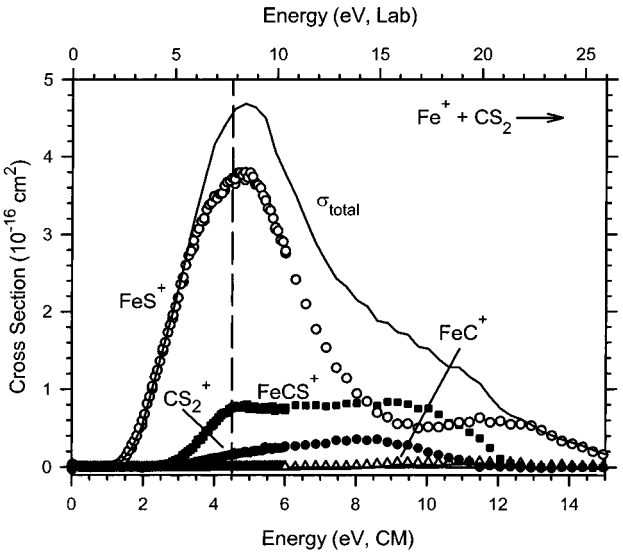

Figure 1. Product cross sections for the formation of FeS^+ (open circles), $FeCS^+$ (closed squares), CS_2^+ (closed circles), and FeC^+ (open triangles) in the reaction of $Fe^+ + CS_2$ as a function of kinetic energy in the center-of-mass (lower axis) and the laboratory (upper axis) frames. The bond dissociation energy of CS_2 (4.50 eV) is marked by the vertical broken line.

Results

Reaction of Fe^+ with CS_2. As noted in our previous work,[13] the main products observed in the reaction of Fe^+ with CS_2 are FeS^+ and $[Fe,C,S]^+$, formed in reactions 2 and 3, respectively. The square brackets around the $[Fe,C,S]^+$ species indicate that the connectivity of the Fe, C, and S atoms is not specified

$$Fe^+ + CS_2 \rightarrow FeS^+ + CS \quad (2)$$

$$\rightarrow [Fe,C,S]^+ + S \quad (3)$$

$$\rightarrow CS_2^+ + Fe \quad (4)$$

$$\rightarrow FeC^+ + S_2 \quad (5)$$

$$\rightarrow FeC^+ + 2S \quad (6)$$

Previously, we showed the cross sections for the products, FeS^+, $[Fe,C,S]^+$, and CS_2^+, up to only 6 eV and limited the discussion to threshold analyses of the two major products.[13] Here, we report these cross sections over a more extended energy range, Figure 1, as obtained using Fe^+ produced in the DC/FT ion source (with methane cooling).

The FeS^+ cross section rises from a threshold near 1.5 eV and continues to rise smoothly until the competitive onset of the $[Fe,C,S]^+$ channel around 2.5 eV. Above 2.5 eV, the FeS^+ cross section rises more slowly because a fraction of the reactive collisions are diverted into the additional reaction pathway associated with $[Fe,C,S]^+$ formation. The lowest-energy threshold of this channel is assigned to the formation of the Fe^+-CS isomer, in which Fe^+ is bound to an intact CS ligand at the carbon end.[24,25] Analysis of the FeS^+ and $[Fe,C,S]^+$ cross

TABLE 2: Optimized Parameters of eq 1

reaction	σ_0	E_0 (eV)	n
$Fe^+ + CS_2 \rightarrow FeS^+ + CS$	2.5 (0.4)	1.44 (0.06)	1.8 (0.1)
$\rightarrow FeCS^+ + S$	0.56 (0.13)	2.35 (0.12)	2.4 (0.2)
$Fe^+ + COS \rightarrow FeS^+ + CO$	2.2 (0.3)	1.16 (0.14)	1.4 (0.2)
$Co^+ + CS_2 \rightarrow CoS^+ + CS$	8.2 (1.1)	1.65 (0.11)	1.2 (0.2)
$\rightarrow CoCS^+ + S$	1.7 (0.5)	1.98 (0.17)	1.6 (0.4)
$Co^+ + COS \rightarrow CoS^+ + CO$	5.2 (0.4)	0.16 (0.05)	0.2 (0.1)

sections using eq 1 yields thresholds of 1.44 ± 0.06 and 2.35 ± 0.12 eV, respectively (Table 2).

Near 4.5 eV, the $[Fe,C,S]^+$ cross section levels out, and the FeS^+ cross section begins to decline. This behavior agrees nicely with the onset of product dissociation according to reaction 7, which has a thermodynamic threshold of 4.50 ± 0.04 eV (Table 1).

$$Fe^+ + CS_2 \rightarrow Fe^+ + S + CS \qquad (7)$$

At slightly higher energies (starting near 5−6 eV), the $[Fe,C,S]^+$ cross section exhibits a second endothermic feature that is poorly resolved from the first. This feature could arise from formation of an excited electronic state of Fe^+−CS or from formation of the metal-inserted C−Fe^+−S isomer. The latter assignment is supported by the observation that a second endothermic feature in the FeS^+ cross section rises near the decline of the $[Fe,C,S]^+$ channel. This correlation suggests that $[Fe,C,S]^+$ is the precursor for FeS^+ at higher energies, consistent with cleaving the SFe^+−C bond of the metal-inserted isomer to yield FeS^+ with isolated C and S atoms according to reaction 8.

$$Fe^+ + CS_2 \rightarrow FeS^+ + C + S \qquad (8)$$

The thermodynamic threshold of 8.8 ± 0.1 eV for reaction 8 (derived from the thermochemistry in Table 1) is reasonably consistent with the FeS^+ cross section (Figure 1), which exhibits a second feature that becomes obvious starting at about 9.5 eV. Additionally, previous studies of the $M^+ + CS_2$ reaction (M = V,[10] Cr,[12] and Mn[12]) are consistent with the formation of a C−M^+−S species at elevated kinetic energies. Despite the arguments supporting the assignment of the second feature of the $[Fe,C,S]^+$ cross section to the formation of the C−Fe^+−S isomer, we cannot definitively exclude the possibility that the formation of an excited state of the Fe^+−CS species or yet another isomer, e.g., Fe^+−SC, is responsible for the observed bimodal behavior.

The FeS^+ cross section declines again starting near 12 eV, in good agreement with the thermodynamic threshold of 11.87 ± 0.06 eV (Table 1) for complete atomization of CS_2 according to reaction 9.

$$Fe^+ + CS_2 \rightarrow Fe^+ + C + 2S \qquad (9)$$

CS_2^+, formed in the charge-transfer reaction 4, is observed as a minor product. The apparent threshold of ~2.5 eV is approximately consistent with the relative ionization energies of Fe (IE = 7.9024 ± 0.0001 eV)[26] and CS_2 (IE = 10.0685 ± 0.0020 eV).[27] The decline in the CS_2^+ product above 9 eV is probably an artifact because this charge-exchange product should have little forward velocity in the laboratory frame such that collection of this ion at high energies may not be efficient. Additionally, minor amounts of FeC^+ with a threshold of 3.6 ± 0.4 eV are also observed. Formation of FeC^+ at these energies must be associated with reaction 5, but only reaches a maximum cross section of 0.01 Å^2. At higher energies, this product cross section increases starting near 8 eV and reaches a maximum of about 0.1 Å^2. The high-energy feature is assigned to reaction 6 as verified by the good agreement with the calculated threshold for reaction 6 of 7.8 ± 0.3 eV (Table 1).

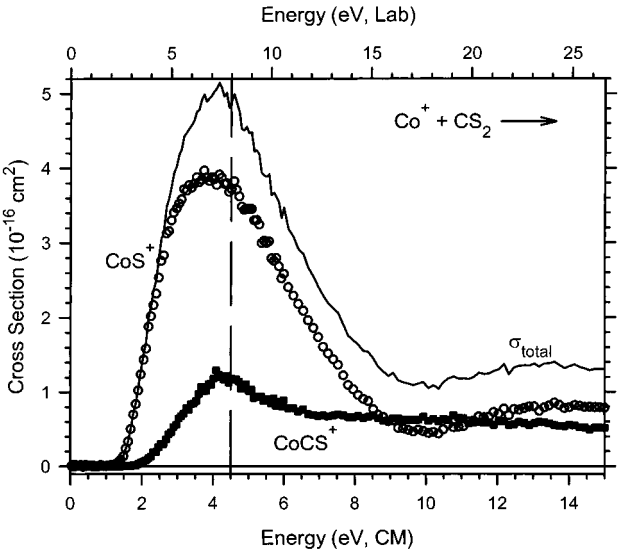

Figure 2. Product cross sections for the formation of CoS^+ (open circles) and $CoCS^+$ (closed squares) in the reaction of $Co^+ + CS_2$ as a function of kinetic energy in the center-of-mass (lower axis) and the laboratory (upper axis) frames. The bond dissociation energy of CS_2 (4.50 eV) is marked by the vertical broken line.

Reaction of Co^+ with CS_2. The product cross sections observed in the reaction of Co^+ with CS_2 are shown in Figure 2. A comparison of the iron and cobalt systems reveals many similarities, such as competition between the two main products, cross sections that peak at 4.5 eV, and a second feature in the CoS^+ cross section that correlates with a decline in the $[Co,C,S]^+$ cross section. These features can be explained by the analogues of reactions 2−9 for Co^+. Let us therefore focus on the differences observed between M = Fe and Co.

Analysis of the CoS^+ cross section using eq 1 yields a threshold of 1.65 ± 0.11 eV, slightly higher than the threshold of 1.44 ± 0.06 eV observed for FeS^+ (Table 2). However, the CoS^+ cross section rises more rapidly than that of FeS^+, thereby reaching its maximum cross section at lower energies, which indicates that CoS^+ formation proceeds more efficiently than FeS^+ formation.[22,28] The difference in slope is evident by inspection of Figures 1 and 2, but also in the optimized values of the fitting parameter *n*, which determines the steepness of the fitting model. For the FeS^+ cross section, *n* is found to be 1.8 ± 0.1, whereas *n* = 1.2 ± 0.2 provides the best fit for the CoS^+ cross section (Table 2). Higher values of *n* correspond to cross sections that rise slowly, which suggests that there are kinetic restrictions along the reaction coordinate in the iron system but not in the cobalt system.

Another difference between the Fe^+/CS_2 and the Co^+/CS_2 systems concerns the behavior of the $[M,C,S]^+$ channels. The magnitude of the $[M,C,S]^+$ channel relative to that of the MS^+ cross section is somewhat larger in the cobalt system. This is partially a consequence of the relatively lower threshold for the $[M,C,S]^+$ channel in the cobalt compared to the iron system, Table 2. Further, although the $[Fe,C,S]^+$ cross section shows evidence of two poorly resolved features of comparable magnitude, the $[Co,C,S]^+$ species does not exhibit obvious bimodal behavior. We believe this is a consequence of the larger $[Co,C,S]^+$ cross section, which obscures the threshold region for the second feature. Nevertheless, after declining from a peak

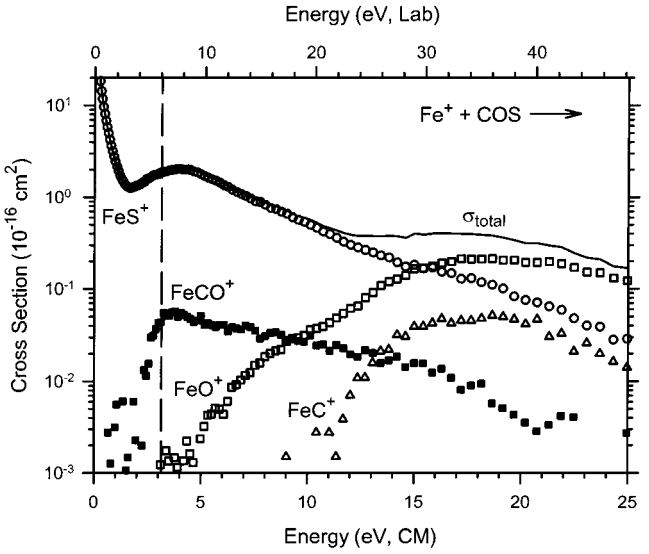

Figure 3. Product cross sections for the formation of FeS^+ (open circles), $FeCO^+$ (closed squares), FeO^+ (open squares), and FeC^+ (open triangles) in the reaction of $Fe^+ + COS$ as a function of kinetic energy in the center-of-mass (lower axis) and the laboratory (upper axis) frames. The bond dissociation energy of OC−S (3.14 eV) is marked by the vertical broken line.

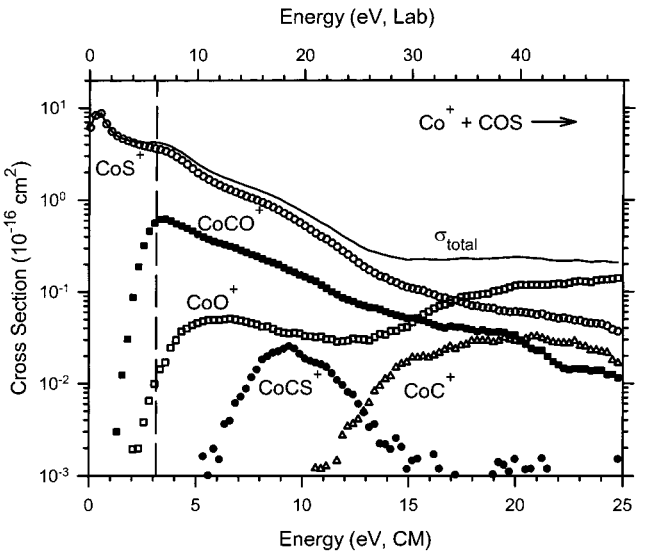

Figure 4. Product cross sections for the formation of CoS^+ (open circles), $CoCO^+$ (closed squares), CoO^+ (open squares), $CoCS^+$ (closed circles) and CoC^+ (open triangles) in the reaction of $Co^+ + COS$ as a function of kinetic energy in the center-of-mass (lower axis) and the laboratory (upper axis) frames. The bond dissociation energy of OC−S (3.14 eV) is marked by the vertical broken line.

near 4.5 eV, the $[Co,C,S]^+$ cross section remains relatively flat over an extended energy range above 7 eV, suggesting that a second feature contributes to the high-energy tail of the $[Co,C,S]^+$ channel.

It is worth commenting on the failure to observe either CS_2^+ or CoC^+ in reactions of Co^+/CS_2 analogous to processes 4−6. Neither of these products was monitored in detail because they were not evident in an initial survey of possible products. This seems reasonable for CoC^+, which in analogy to the Fe^+/CS_2 system, is likely to have a very small cross section. However, it is unlikely that the CS_2^+ charge transfer product was inadvertently missed if its cross section is comparable to that observed in the Fe^+/CS_2 system. An explanation for the failure to observe this product is discussed below.

Reactions with COS. The product cross sections observed in the reactions of Fe^+ and Co^+ with COS are shown in Figures 3 and 4, respectively. One of the most pronounced differences between the CS_2 and COS systems is the behavior of the MS^+ channel. The C−S bond energy in COS is lower than in CS_2 (by 1.36 eV, Table 1), which shifts the thresholds of the MS^+ cross sections to lower energies in the reactions with COS. From the measured thresholds in the CS_2 systems, we calculate that the thresholds for reactions 10 and 11,

$$Fe^+ + COS \rightarrow FeS^+ + CO \qquad (10)$$

$$Co^+ + COS \rightarrow CoS^+ + CO \qquad (11)$$

should appear at 0.08 ± 0.09 and 0.27 ± 0.11 eV, respectively. Using eq 1, the threshold of reaction 11 is determined to be 0.16 ± 0.05 eV. This value is in reasonable agreement with the thermochemistry derived from the CS_2 reaction. The cross section for FeS^+ formation according to reaction 10 exhibits no obvious threshold, consistent with an approximately thermoneutral process. Indeed, our cross section for this process can be converted[16] to a rate constant of $(3.5 \pm 0.7) \times 10^{-10}$ cm^3 $molecule^{-1}$ s^{-1}, which compares favorably to a previous ion cyclotron resonance (ICR) measurement of the room-temperature rate constant, $(2.6 \pm 1.1) \times 10^{-10}$ cm^3 $molecule^{-1}$ s^{-1}.[13] In addition, equilibrium at room temperature was established for reaction 10, and the equilibrium constant was converted to an endothermicity of 0.06 ± 0.04 eV for reaction 10. An interesting aspect of this process is that the products of reaction 10 have twice as many rotations as the reactants, such that entropic effects lead to exoergic behavior for reaction 10 at room temperature. The temperature of the COS reactant in our experiments is ~300 K, so exoergic behavior is also expected in our experiments.

The FeS^+ cross section exhibits a distinct endothermic feature near 1.5 eV, indicating that an additional pathway for FeS^+ formation has become available. The CoS^+ cross section also shows an endothermic feature in this region, but it is not as pronounced. The onset of a higher-energy pathway for FeS^+ formation must be attributed either to the formation of a different set of neutral products, the formation of electronically excited product states, or a new pathway to the ground-state products that proceeds over a barrier. The threshold for forming FeS^+ along with isolated C and O atoms according to reaction 12,

$$Fe^+ + COS \rightarrow FeS^+ + C + O \qquad (12)$$

is calculated to be 11.17 ± 0.04 eV (Table 1), much too high to account for the observed behavior. Formation of the first excited state of CO requires 6.04 eV,[29] making its formation energetically inaccessible as well.

We next consider whether the second feature in the FeS^+ cross section can be attributed to formation of electronically excited FeS^+. The threshold of the second feature is estimated by subtracting a power law fit of the low-energy feature from the data and modeling the remainder using eq 1. This process is somewhat speculative, because the exact energy dependence of the low-energy process above 1 eV is unknown. Nevertheless, a range of reasonable behaviors for the low-energy feature can be subtracted from the data to establish several approximations of the isolated higher-energy process. Using this approach, we analyze the high-energy feature using eq 1 to obtain a threshold of 1.16 ± 0.14 eV. According to Table 1, the thermodynamic threshold for $FeS^+(^6\Sigma^+)$ formation in reaction 10 is 0.06 ± 0.04 eV. Thus, the adiabatic excitation energy from the $FeS^+(^6\Sigma^+)$ state to the purported excited state of FeS^+ amounts to $1.10 \pm$

0.15 eV. To examine what states might be responsible for this feature, we rely on calculations of Harvey et al. performed at the averaged coupled-pair functional (ACPF) level of theory where only the valence electrons were correlated.[30] These calculations obtain a $^6\Sigma^+$ ground-state having a bond energy of 2.83 eV, 0.25 eV lower in energy than our experimental value. Excited states include $^4\Pi$ and $^4\Phi$ states, both having $1\sigma^2 2\sigma^2 1\pi^4 1\delta^3 3\sigma^1 2\pi^1$ configurations, that lie 0.34 and 0.37 eV above the $^6\Sigma^+$ ground state. Two $^4\Delta$ states, having $1\sigma^2 2\sigma^2 1\pi^4 1\delta^3 3\sigma^0 2\pi^2$ and $1\sigma^2 2\sigma^2 1\pi^4 1\delta^2 3\sigma^1 2\pi^2$ configurations, are close in energy with the latter lying 0.75 eV above the ground state. Another $^4\Pi$ state having a $1\sigma^2 2\sigma^2 1\pi^4 1\delta^2 3\sigma^2 2\pi^1$ configuration should also exist, but was not included in the calculations. None of these excitation energies agrees particularly well with the measured energy difference between the two features in the FeS^+ cross section. Moreover, any assignment of the high-energy feature to one of the quartet states of FeS^+ leaves it unclear why other quartet states would not be observed experimentally. Therefore, we consider occurrence of a second pathway to formation of ground-state products to be a more likely explanation for the second feature. The plausibility of this assignment as a pathway involving only a sextet surface is discussed further below.

In addition to the formation of the MS^+ species, many other product channels are observed in the $M^+ + COS$ reactions. At low energies, MS^+ and MCO^+ are observed, analogous to the formations of MS^+ and MCS^+ in the reactions with CS_2. This behavior is consistent with insertion of M^+ into the OC−S bond to form the OC−M^+−S intermediate (although direct S atom abstraction from COS could also contribute to the observed MS^+ cross sections). Note that both MCO^+ cross sections begin to decline at the bond energy of OC−S, indicating the opening of the decomposition channel $M^+ + CO + S$. At higher energies, the much stronger SC−O bond may be activated to form the SC−M^+−O intermediate. Decomposition of this intermediate leads to the formation of MO^+ and MCS^+. Unfortunately, the $FeCS^+$ channel was not monitored in the Fe^+/COS system, because this product was not evident in an initial survey of possible products. Given the similarities between the other cross sections in the Co^+/COS and Fe^+/COS systems, it seems likely that the $FeCS^+$ species is formed in the reaction with COS. However, on the basis of the differences in the MCS^+ cross sections observed in the CS_2 systems, we anticipate that the $FeCS^+$ cross section is probably smaller than that shown for $CoCS^+$ in Figure 4, consistent with our failure to observe $FeCS^+$ in our initial product survey. As shown in Figures 3 and 4, the magnitudes of the MS^+ and MCO^+ cross sections are larger than those of the MO^+ and MCS^+ cross sections at energies below 15 eV. Clearly, activation of the weaker OC−S bond is preferred over SC−O activation at lower energies. This difference in bond strength is also responsible in part for the observation that the MS^+ and MCO^+ channels appear at lower energies than the MO^+ and MCS^+ products.

Beginning near 11 eV in both systems, the formation of MC^+ is observed. Given the MC^+ bond energies in Table 1,[31,32] the observed thresholds are consistent with the formation of $MC^+ + O + S$, which are calculated to begin at 10.17 ± 0.30 and 10.65 ± 0.30 eV for M = Fe and Co, respectively. Thus, these products could arise from dissociation of either the MCO^+ or MCS^+ species. Although the energetic requirements for MC^+ formation are the same for both precursors, Figure 4 shows that the rise of the CoC^+ channel appears correlated predominantly with the decline of the $CoCS^+$ channel. Considering the relative bond strengths in these species, it is not surprising that MCS^+ might decompose more readily to MC^+ than MCO^+ does. To form MC^+ from MCX^+ (X = O, S), the C−X bond must be ruptured while leaving the M^+−C bond intact, a process that appears to be easier when X = S because the C−O bond is stronger than the C−S bond.

Finally, both the FeO^+ and CoO^+ channels exhibit two endothermic features. The low energy thresholds for MO^+ generation (Figures 3 and 4) are reasonably consistent with reactions 13 and 14

$$Fe^+ + COS \rightarrow FeO^+ + CS \quad (13)$$

$$Co^+ + COS \rightarrow CoO^+ + CS \quad (14)$$

which have thermodynamic thresholds of 3.41 ± 0.07 and 3.63 ± 0.06 eV, respectively (calculated using information in Table 1). Note that the CoO^+ cross section rises much more rapidly from threshold compared to the FeO^+ cross section, an observation that is another example of a kinetic restriction operative in the latter system.[33,34]

Formation of MO^+ with isolated C and S atoms requires an additional energy of 7.37 ± 0.04 eV = D(CS). Therefore, the thermodynamic thresholds for reactions 15 and 16

$$Fe^+ + COS \rightarrow FeO^+ + C + S \quad (15)$$

$$Co^+ + COS \rightarrow CoO^+ + C + S \quad (16)$$

are 10.78 ± 0.08 and 11.00 ± 0.07 eV, respectively. These values are approximately consistent with the observed thresholds of the second features in the MO^+ cross sections. Hence, the low-energy formations of MO^+ are assigned to reactions 13 and 14 and the high-energy routes to reactions 15 and 16. The dominance of the latter channels above about 15 eV may be attributed to the fact that the MO^+ bond energies are stronger than the MS^+ bond energies. However, the observation of such products at very high energies suggests that they may be formed in impulsive (stripping) collisions,[35] which tend to leave considerable amounts of energy in translation of the products, thereby allowing stable molecular products. In addition, such impulsive collisions favor transfer of light atoms (here, O vs S).[35]

Thermochemistry. From the threshold of 1.44 ± 0.06 eV (Table 2) for forming FeS^+ in reaction 1, we calculate $D_0(Fe^+-S) = 3.06 \pm 0.07$ eV. This value agrees well with the apparent thermoneutral formation of the FeS^+ species in the reaction with COS, which implies that $D_0(Fe^+-S)$ is close in energy to D_0(OC−S) = 3.14 eV. Combined with the results of ion/molecule equilibria studies,[13] a final value of $D_0(Fe^+-S) = 3.08 \pm 0.04$ eV is obtained (Table 1), one of the most precisely known binding energies of a transition-metal compound.

The cross section for forming the CoS^+ product in the CS_2 system was analyzed using eq 1 yielding a threshold of 1.65 ± 0.11 eV, Table 2. Combined with $D_0(SC-S) = 4.50 \pm 0.04$ eV, we determine $D_0(Co^+-S) = 2.85 \pm 0.11$ eV. An independent measure of $D_0(Co^+-S)$ can be obtained by analysis of the CoS^+ cross section in the reaction with COS. The threshold for this process is 0.16 ± 0.05 eV (Table 2), which leads to $D_0(Co^+-S) = 2.98 \pm 0.05$ eV. The weighted average[36] of the CoS^+ bond energies calculated from these two reactions results in a final estimate of $D_0(Co^+-S) = 2.95 \pm 0.09$ eV, where the uncertainty is conservatively estimated as two standard deviations of the mean.

From the respective thresholds of 2.35 ± 0.12 and 1.98 ± 0.17 eV associated with forming $FeCS^+$ and $CoCS^+$ in the

reactions with CS_2, we calculate $D_0(Fe^+-CS) = 2.15 \pm 0.13$ (reported in reference 13) and $D_0(Co^+-CS) = 2.52 \pm 0.18$ eV. Previously, [13] we also determined $D_0(Fe^+-CS) = 2.40 \pm 0.12$ eV from the reaction $FeS^+ + CS_2 \rightarrow FeCS^+ + S_2$ and explained the discrepancy by noting that formation of $FeCS^+$ (reaction 3) has a higher threshold than FeS^+ formation via reaction 2. Because formation of FeS^+ is the dominant pathway for reaction, competition between these channels may cause the measured threshold of the less efficient $FeCS^+$ channel to be somewhat elevated. It is possible that similar competition occurs in the cobalt system, although any competitive shift should be less than in the iron system because the thresholds for MS^+ and MCS^+ formation are much closer together for Co^+ (difference of 0.33 ± 0.20 eV, Table 2) compared to Fe^+ (0.91 ± 0.13 eV, Table 2). In addition, reaction 3 and its cobalt analogue have different electronic spin considerations, as discussed further below, that could change the extent of competition in the iron and cobalt systems. Nevertheless, the Co^+-CS bond energy of 2.52 ± 0.18 eV is most conservatively viewed as a lower limit. A reasonable upper limit comes by assuming that the competitive shift in this threshold is no larger than in the iron system, 0.25 ± 0.18 eV, such that $D_0(Co^+-CS) \leq 2.77 \pm 0.25$ eV. Combining the upper and lower limits gives a Co^+-CS bond energy that can be assigned as 2.68 ± 0.34 eV, where the uncertainty spans the range of possible values.

Discussion

Thermochemistry of Metal Sulfide Cations. The 0 K metal-sulfide cation bond energy for cobalt is derived here from the reactions of Co^+ with CS_2 and COS as 2.95 ± 0.09 eV. Similarly, guided ion beam studies combined with ICR results reported previously[13] lead to $D_0(Fe^+-S) = 3.08 \pm 0.04$ eV. These values can be converted to 298 K values using frequency calculations performed at the B3LYP/6-311+G* level which find 463 cm^{-1} for FeS^+ and 419 cm^{-1} for CoS^+.[8] In both cases, the correction from 0 to 298 K is 0.03 eV giving 3.11 ± 0.04 and 2.98 ± 0.09 eV, respectively, as the 298 K bond energies. These values are higher than previous determinations of these bond energies using photodissociation: 2.81 ± 0.22[37] and 2.65 ± 0.26[38] eV for FeS^+ and 2.69 ± 0.22 eV[37] for CoS^+. The ability to establish an equilibrium for reaction 10 and the excellent agreement between the thermochemistry derived from this equilibrium and the threshold for reaction 2 make it unambiguous that the FeS^+ bond energy is near that of D(OC−S) = 3.14 eV. Likewise, the cross section behavior for the CoS^+ product formed in the Co^+/COS system is inconsistent with a threshold of 0.45 ± 0.22 eV, as derived from a 2.69 ± 0.22 eV bond energy. Therefore, the photodissociation results must be lower limits, which can be the result of (i) internally excited ions, (ii) multiphoton processes, and/or (iii) the imperfect step function of the cutoff filters used in these experiments.

The FeS^+ bond energy is slightly larger than that of CoS^+, by 0.13 ± 0.10 eV (Table 1). A similar trend has been observed for the oxides of these metals: $D_0(Fe^+-O) = 3.47 \pm 0.06$[39,40] and $D_0(Co^+-O) = 3.25 \pm 0.05$ eV.[34,40,41] To understand these differences, consider the valence molecular orbitals that arise in these molecules using LCAO-MO theory. To a first approximation (considering only valence electrons), the 3s orbital of sulfur (2s on oxygen) constitutes the 1σ orbital, the 4s and 3d orbitals on the metal combine with the 3p orbitals on sulfur (2p on oxygen) to form 2σ and 1π bonding orbitals, 1δ and 3σ nonbonding orbitals, and 2π and 4σ antibonding orbitals. The ground states of FeS^+ and FeO^+ are found to be high-spin $^6\Sigma^+$ states with $1\sigma^2 2\sigma^2 1\pi^4 1\delta^2 3\sigma^1 2\pi^2$ electron configurations.[8,30,42−44] Because the 1δ, 3σ, and 2π orbitals are close in energy, the high-spin configuration is preferred in order to maximize the electron exchange energy. The addition of another electron for Co^+ results in a $1\sigma^2 2\sigma^2 1\pi^4 1\delta^3 3\sigma^1 2\pi^2$ electron configuration and a $^5\Delta$ ground state.[43,44] Although the formal bond order is two in both cases, the slightly weaker bond for Co vs Fe can be rationalized by the loss of exchange energy associated with the lower spin state.

Thermochemistry of Metal Thio-carbonyl Cations. The observed trend in the relative bond strengths of $FeCS^+$ and $CoCS^+$ (Table 1) is consistent with the previously measured thermochemistry of the analogous carbonyl species.[40,45−47] The weaker Fe^+-CX bonds can be explained by considering the potential-energy surfaces for dissociation of the $FeCX^+$ and $CoCX^+$ molecules (X = O, S). Because the ^3F ground state of Co^+ has a $3d^8$ configuration, the electron pair in the highest occupied molecular orbital (HOMO) of CX can be donated into the empty 4s orbital of Co^+, resulting in an attractive interaction and a strong dative bond. The $Co^+(^5F)$ first excited state, however, has a $4s^1 3d^7$ configuration, which leads to a more repulsive interaction between Co^+ and CX. Therefore, the ground states of the $CoCX^+$ species are certainly triplets[48] and correlate adiabatically and diabatically with the $Co^+(^3F) + CX(^1\Sigma^+)$ ground-state product fragments. That is, dissociation of $CoCX^+$ occurs on a single potential energy surface.

Unlike $CoCX^+$, $FeCX^+$ molecules have more complicated potential energy surfaces. Ground states of the $FeCX^+$ species are likely to be quartets, arising from the interaction of excited-state $Fe^+(^4F, 3d^7)$ with $CX(^1\Sigma^+)$.[48] The $3d^6 4s^1$ electron configuration of the $Fe^+(^6D)$ ground-state results in less attractive interactions with CX. Therefore, the lowest energy (adiabatic) dissociation of $FeCX^+$ involves a crossing from a quartet to a sextet surface. If we calculate diabatic bond dissociation energies (D_d) for $FeCX^+$ on the quartet surface using the $Fe^+(^4F) \leftarrow Fe^+(^6D)$ excitation energy of 0.25 eV,[26] we obtain $D_d(Fe^+-CS) = 2.65 \pm 0.12$ eV and $D_d(Fe^+-CO) = 1.61 \pm 0.08$ eV. These values are now comparable to the values for $D_0(Co^+-CS) = 2.68 \pm 0.34$ eV and $D_0(Co^+-CO) = 1.80 \pm 0.07$ eV.

Reaction Mechanism. The initial species formed in the interaction of a metal ion with CS_2 is a simple adduct, as demonstrated in ab initio calculations of the V^+/CS_2 potential energy surface.[10] This is also consistent with the identification of a symmetrically bound $Co^+(CS_2)$ complex in the low temperature, matrix isolation IR spectroscopy work of Zhou and Andrews as well as their theoretical work on the isolated complex.[15] For processes 2, 3, and the cobalt analogues to occur, the next step in these reactions must be insertion of the metal cation into one of the C−S bonds to form $S-M^+-C-S$ intermediates. Results of the analogous V^+, Cr^+, and Mn^+ reactions with CS_2 are consistent with the formation of a $S-M^+-C-S$ intermediate,[10,12] as are ab initio calculations of the V^+/CS_2 potential energy surface.[10] All of the observed products can be formed by cleavage of specific bonds of this intermediate. Thus, cleavages of the SM^+-CS and $S-MCS^+$ bonds lead to the low-energy formations of MS^+ and MCS^+ according to reactions 2 and 3 and the cobalt analogues, respectively. Cleavage of the SMC^+-S bond leads to the inserted $S-M^+-C$ species, which can further decompose to yield MS^+. The small amount of FeC^+ formed in reaction 6 of the Fe^+/CS_2 system is also consistent with decomposition of $S-Fe^+-C$. If our assignment of the second feature to the metal-inserted $S-M^+-C$ isomer is correct, our observations indicate that the Fe^+-CS and $C-Fe^+-S$ isomers are formed with comparable efficiencies (judging by the magnitude of their

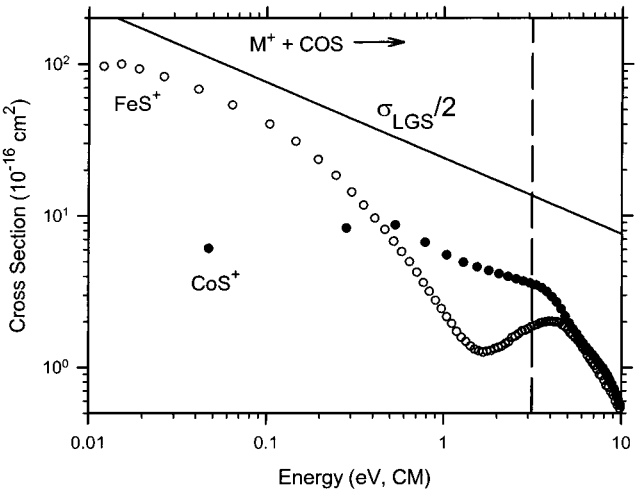

Figure 5. Product cross sections for the formation of FeS^+ (open circles) and CoS^+ (closed circles) in the reactions of $M^+ + COS$ as a function of kinetic energy in the center-of-mass frame. The line is half the Langevin−Gioumousis−Stevenson collision rate, ref 49. The bond dissociation energy of OC−S (3.14 eV) is marked by the vertical broken line.

respective cross sections), whereas the $C-Co^+-S$ isomer is formed much less efficiently than Co^+-CS. Note that the former species is the likely precursor to CoC^+ formation in the reaction analogous to process 6, thereby providing a partial explanation for the failure to observe CoC^+ in the Co^+/CS_2 system.

Analogous mechanisms in the COS systems explain the experimental observations. Here, insertion into the C−S bond is more facile than in CS_2 because the bond is weaker. However, there is a substantially reduced probability of inserting into the C−O bond to form the $O-M^+-C-S$ intermediate, because of the large difference in the C−O and C−S bond energies. Thus, MS^+ and MCO^+ dominate the products at low energies, whereas MO^+ and MCS^+ are formed as minor products. At high energies, formations of MO^+ according to reactions 15 and 16 dominate, most likely because of impulsive behavior (see above).

Differences in Reactivities. The FeS^+ and CoS^+ cross sections illustrate an important distinction between thermodynamics and kinetics. The FeS^+ cross section rises from a slightly lower threshold than CoS^+ (Table 2), because of the stronger FeS^+ bond energy. Nevertheless, once it becomes energetically accessible, the CoS^+ cross section rises more rapidly than the FeS^+ cross section, apparently because it is less hindered. These two effects compensate such that the overall magnitude of the cross sections in the CS_2 systems is comparable for both metal ions. The COS systems also show notable differences in reactivity. Figure 5 compares the cross sections for reactions 10 and 11 along with the collision cross section.[49−51] It can be seen that even though the efficiency of the iron reaction far exceeds that for cobalt at the lowest energies, again a consequence of the weaker CoS^+ bond energy, the efficiency of reaction 11 is higher at energies above about 0.5 eV. These results are surprising because the formation of ground-state FeS^+ in reactions 17 is spin-allowed, whereas the formation of ground-state CoS^+ in reactions 18 is spin-forbidden.

$$Fe^+ (^6D) + CXS (^1\Sigma_g^+) \rightarrow FeS^+ (^6\Sigma^+) + CX (^1\Sigma^+) \quad (17)$$

$$Co^+ (^3F) + CXS (^1\Sigma_g^+) \rightarrow CoS^+ (^5\Delta) + CX (^1\Sigma^+) \quad (18)$$

Some of the differences in the two metal systems can be attributed to the ground-state configurations of $Fe^+(^6D, 4s^13d^6)$ and $Co^+(^3F, 3d^8)$. Occupation of the spherical 4s orbital in $Fe^+(^6D)$ hinders the interaction between Fe^+ and CXS, thereby disfavoring the formation of the insertion intermediate, $S-Fe^+-CX$. Because the 4s orbital is empty in $Co^+(^3F)$, there is no such inhibition in the cobalt system. A related explanation involves the spin state of the $S-M^+-CX$ intermediate, which may be estimated by considering the interaction of MS^+ with the CS ligand. The $FeS^+(^6\Sigma^+, 1\sigma^22\sigma^21\pi^41\delta^23\sigma^12\pi^2)$ and $CoS^+(^5\Delta, 1\sigma^22\sigma^21\pi^41\delta^33\sigma^12\pi^2)$ ground states have no low-lying empty orbitals into which the electron pair on the CS ligand can be donated. However, quartet states of FeS^+ and triplet states of CoS^+ can have configurations with an empty orbital that can accept the electron pair of the CS ligand. (For example, a 3σ or 2π electron can be excited to one of the 1δ orbitals to yield $^4\Delta$ or $^4\Phi/\Pi$ states for FeS^+ and $^3\Sigma^-$ or $^3\Pi$ states for CoS^+.) Additionally, π-back-bonding from the electrons in the 2π molecular orbitals of MS^+ can strengthen the metal-to-carbon interaction. Therefore, it is likely that the ground states of the $S-M^+-CX$ intermediates are a quartet for iron and a triplet for cobalt. For iron, forming the quartet intermediate from ground-state reactants is spin-forbidden, whereas for cobalt, it is spin-allowed. For both metals, formation of ground-state products from the low-spin intermediate is spin-forbidden. Therefore, even though the overall reaction 17 is spin-allowed, it probably undergoes spin-inversion twice along the reaction coordinate, and is essentially *doubly* spin-forbidden. These spin constraints, combined with the more repulsive effects of the 4s electron of $Fe^+(^6D)$, probably account for the apparent kinetic restrictions operative in reactions 17 compared to reactions 18 with X = O and S.

Spin may also play a role in the relative efficiencies for formation of $MCS^+ + S$, which can be described by reactions 19 and 20 (X = S). We again presume that the reactions take place via $S-M^+-CS$ intermediates of quartet and triplet spin, respectively.

$$Fe^+ (^6D) + CXS (^1\Sigma_g^+) \rightarrow FeCS^+ (^4\Sigma^+) + X (^3P) \quad (19)$$

$$Co^+ (^3F) + CXS (^1\Sigma_g^+) \rightarrow CoCS^+ (^3\Delta) + X (^3P) \quad (20)$$

In contrast to reactions 18, reactions 20 are spin-allowed throughout, such that competition between the MS^+ and MCS^+ channels in the CS_2 systems is likely to be less important for M = Co than M = Fe. Support for this conclusion comes from the significantly lower value of n for reaction 20 compared to 19 (X = S, Table 2). Accordingly, it is possible that the threshold measured for reaction 20 is a reasonable measure of the thermodynamic threshold rather than an upper limit; notwithstanding, we conservatively keep $D_0(Co^+-CS) = 2.68 \pm 0.34$ eV as our best experimental value. In contrast, although the overall reactions 19 are spin-allowed, the energetically lowest pathway probably involves the $S-M^+-CS$ quartet intermediate, making the process spin-forbidden in the first step and therefore subject to the kinetic restrictions discussed above.

Another difference in the reactivities of Fe^+ and Co^+ with CS_2 involves the charge-transfer reaction, which occurs with a reasonable cross section for iron, process 4, but is not observed for cobalt. There are two interrelated effects that explain these observations. For reaction of $Fe^+(^6D, 4s^13d^6)$, removal of an electron from CS_2 can form the $Fe(^5D, 4s^23d^6)$ ground state in a spin-allowed process. Therefore, charge transfer competes favorably with the other kinetically restricted channels, reactions 2 and 3. In the cobalt system, addition of an electron to Co^+-

(^3F, $3d^8$) cannot form the Co(^4F, $4s^23d^7$) ground state without moving electrons around. The first one-electron charge-transfer process that is available would form the Co(^4F, $4s^13d^8$) first excited state, 0.43 eV higher in energy.[26] Thus, single electron transfer is energetically less favorable in the cobalt system and competes with reactions that are more efficient than in the iron system. Apparently, these factors make the charge-transfer reaction between Co^+ and CS_2 inefficient enough that its cross section is fairly small.

Multiple Pathways for Fe^+/COS. The postulated quartet intermediate for reaction of Fe^+ with COS can now help explain the observation of the second feature in the FeS^+ cross section, Figure 3. As noted above, this feature can neither be attributed to formation of a different neutral product nor to excited states of CO or FeS^+. However, if the thermoneutral reaction proceeds through an intermediate having quartet spin, the sextet reactants must undergo spin inversion to reach this intermediate, and then again to reach the FeS^+ ($^6\Sigma^+$) ground-state products. At higher energies, a sextet intermediate may be accessed, circumventing both spin restrictions. This would result in increased reaction efficiency and could lead to a distinct endothermic feature, where the threshold corresponds to the height of the limiting barrier along the sextet surface. A similar competition of a low-energy pathway associated with two spin changes and a second, spin-allowed route at elevated energies has also been suggested to explain the observations in the reactions of FeS^+ with H_2.[14]

The presence of two pathways for production of FeS^+ in the COS system indicates that the low-energy part of the FeS^+ cross section observed in the Fe^+/CS_2 system might also consist of two features. However, the threshold for forming FeS^+ from CS_2 is higher in energy in comparison to COS. The higher threshold in the CS_2 reaction causes the formation of both FeS^+ states to be endothermic, rendering them indistinct. Presumably, the different energy dependences of the processes for FeS^+ formation in the Fe^+/COS reaction (one is approximately thermoneutral, and the other is endothermic) contribute to their being discernible from one another. In the cobalt system, the metal ion reactant already has the same low-spin state as the intermediate, such that there is no spin-allowed pathway to form ground-state products starting from ground-state reactants, even at higher energies. However, low-lying triplet states of CoS^+ are expected to exist and could presumably be formed by spin-allowed dissociation of the $SCoCX^+$ intermediates. This may explain the small features in the CoS^+ cross section in the COS system observed at slightly higher energies near 3 eV.

Summary

The kinetic-energy dependences of the reactions of Fe^+ and Co^+ with CS_2 and COS are examined using guided ion beam mass spectrometry. The results of these reactions are consistent with the initial formation of the metal-inserted $X-M^+-C-X$ intermediate species (X = S, O). The $FeCS^+$ cross section observed in the Fe^+/CS_2 reaction exhibits two features that are attributed to the formation of the Fe^+-CS and $S-Fe^+-C$ isomers that arise from different fragmentations of the $S-Fe^+-C-S$ intermediate. In the $M^+ + COS$ reactions, the MS^+ and MCO^+ products appear at lower energies and have larger cross section magnitudes than the MO^+ and MCS^+ products, indicating that activation of the weaker C−S bond of the COS molecule is preferred. It is anticipated that the $X-M^+-C-X$ intermediates are low-spin in both metal systems, such that formation of ground-state MS^+ and MO^+ products requires two spin changes for iron and only one for cobalt. This can explain differences in the relative efficiencies observed in the two metal cation systems.

The FeS^+ cross section observed in the COS reaction exhibits two features that are assigned to the formation of FeS^+ along two pathways. One of them involves two surface crossings and the ground-state quartet $SFeCO^+$ intermediate, whereas the other proceeds entirely along a sextet surface. From the threshold of the higher energy feature, we estimate the barrier along the sextet surface to be 1.10 ± 0.15 eV relative to the reactants. A distinct endothermic cross section feature probably arises because spin is conserved, in contrast to the lower energy pathway that requires crossing between sextet reactants to a proposed quartet $S-Fe^+-CO$ intermediate and then back to sextet products.

Finally, from the thresholds associated with forming CoS^+ and $CoCS^+$, we determine 0 K bond energies of $D_0(Co^+-S) = 2.95 \pm 0.09$ and $D_0(Co^+-CS) = 2.68 \pm 0.34$ eV, which can be compared with the previously reported values: $D_0(Fe^+-S) = 3.08 \pm 0.04$ and $D_0(Fe^+-CS) = 2.40 \pm 0.12$ eV.[13]

Acknowledgment. This work is supported by the National Science Foundation, Grant No. CHE-9877162. The Berlin group acknowledges support by the Deutsche Forschungsgemeinschaft, the Volkswagen-Stiftung, and the Fonds der Chemischen Industrie.

References and Notes

(1) Stiefel, E. I. In *Transition Metal Sulfur Chemistry*; Stiefel, E. I.; Matsumoto, K. Eds.; ACS Symposium Series 653. American Chemical Society: Washington, DC, 1996; pp 2−38, and references therein.
(2) Takakuwa, S. In *Organic Sulfur Chemistry, Biochemical Aspects*; Oae, S.; Okyama, T., Eds.; CRC Press: Boca Raton, FL, 1992.
(3) Lippard, S. J.; Berg, J. M. *Principles of Bioinorganic Chemistry*; University Science Books: Mill Valley, CO., 1994.
(4) Rehder, D. *Angew. Chem., Int. Ed. Engl.* **1991**, *30*, 148.
(5) Butler, A.; Carrano, C. J. *Coord. Chem. Rev.* **1991**, *109*, 61.
(6) Holm, R. H. *Chem. Rev.* **1996**, *96*, 2237.
(7) Curtis, M. D. In *Transition Metal Sulfur Chemistry*; Stiefel, E. I., Matsumoto, K., Eds.; ACS Symposium Series 653. American Chemical Society: Washington, DC, 1996; pp 154−175.
(8) For a general discussion of the periodic trends of first and second-row transition-metal sulfides, see: Kretzschmar, I. Ph.D. Thesis, Technische Universität Berlin D83, 1999. Published as *Energetics and Reactivity of the Binary Transition-Metal Sulfides of the 3rd and 4th Row*; Shaker Verlag: Aachen, 1999.
(9) Kretzschmar, I.; Schröder, D.; Schwarz, H.; Rue, C.; Armentrout, P. B. *J. Phys. Chem. A* **2000**, *104*, 5046.
(10) Rue, C.; Armentrout, P. B.; Kretzschmar, I.; Schröder, D.; Harvey, J. N.; Schwarz, H. *J. Chem. Phys.* **1999**, *110*, 7858.
(11) Kretzschmar, I.; Schröder, D.; Schwarz, H.; Rue, C.; Armentrout, P. B. *J. Phys. Chem.* **1998**, *102*, 10 060.
(12) Rue, C.; Armentrout, P. B.; Schröder, D.; Kretzschmar, I.; Schwarz, H. *Int. J. Mass Spectrom.* **2001**, in press.
(13) Schröder, D.; Kretzschmar, I.; Schwarz, H.; Rue, C.; Armentrout, P. B. *Inorg. Chem.* **1999**, *38*, 3474.
(14) Bärsch, S.; Kretzschmar, I.; Schröder, D.; Schwarz, H.; Armentrout, P. B. *J. Phys. Chem. A* **1999**, *103*, 5925.
(15) Zhou, M.; Andrews, L. *J. Phys. Chem. A* **2000**, *104*, 4394.
(16) Ervin, K. M.; Armentrout, P. B. *J. Chem. Phys.* **1985**, *83*, 166.
(17) Schultz, R. H.; Armentrout, P. B. *Int. J. Mass Spectrom. Ion Processes* **1991**, *107*, 29.
(18) (a) Khan, F. A.; Steele, D. L.; Armentrout, P. B. *J. Phys. Chem.* **1995**, *99*, 7819. (b) Chen, Y.-M.; Armentrout, P. B. *J. Chem. Phys.* **1995**, *103*, 618. (c) Fisher, E. R.; Kickel, B. L.; Armentrout, P. B. *J. Chem. Phys.* **1992**, *97*, 4859. (d) Kemper, P. R.; Bowers, M. T. *J. Phys. Chem.* **1991**, *95*, 5134.
(19) Clemmer, D. E.; Chen, Y.-M.; Khan, F. A.; Armentrout, P. B. *J. Phys. Chem.* **1994**, *98*, 6522.
(20) Haynes, C. L.; Armentrout, P. B. *Organometallics* **1994**, *13*, 3480.
(21) Gerlich, D. In *State-Selected and State-to-State Ion−Molecule Reaction Dynamics, Part 1: Experiment*; Ng, C. Y., Baer, M., Eds.; Advances in Chemical Physics Series, Vol. LXXXII (John Wiley & Sons Inc., 1992), pp 1−176.
(22) Armentrout, P. B. In *Advances in Gas-Phase Ion Chemistry*; Adams, N. G., Babcock, L. M., Eds.; JAI: Greenwich, 1992; Vol. 1, pp 83−119.
(23) Armentrout, P. B. *Int. J. Mass Spectrom.* **2000**, *200*, 219.
(24) Mavridis, A.; Harrison, J. F.; Allison, J. *J. Am. Chem. Soc.* **1989**, *111*, 2482.
(25) Jeung, G.-H. *Chem. Phys. Lett.* **1994**, *221*, 237.

(26) Sugar, J.; Corliss, C. *J. Phys. Chem. Ref. Data* **1985**, *14*, Supple. No. 2, 1.

(27) Lias, S. G.; Bartmess, J. E.; Liebman, J. F.; Holmes, J. L.; Levin, R. D.; Mallard, W. G. *J. Phys. Chem. Ref. Data* **1988**, *17*, Supple. No. 1, 1.

(28) Armentrout, P. B. In *Structure/Reactivity and Thermochemistry of Ions*, Ausloos, P.; Lias, S. G., Eds.; D. Reidel: Dordrecht, 1987; pp 97−164.

(29) Huber, K. P.; Herzberg, G. *Molecular Spectra and Molecular Structure. IV. Constants of Diatomic Molecules*; Van Nostrand Reinhold: New York, 1979; p 166.

(30) Harvey, J. N.; Heinemann, C.; Fiedler, A.; Schröder, D.; Schwarz, H. *Chem. Eur. J.* **1996**, *2*, 1230.

(31) Hettich, R. L.; Freiser, B. S. *J. Am. Chem. Soc.* **1986**, *106*, 2537.

(32) Haynes, C. L.; Chen, Y.-M.; Armentrout, P. B. *J. Phys. Chem.* **1995**, *99*, 9110.

(33) The threshold measured for the CoO^+ cross section is lower than the thermodynamic threshold for reasons that are unclear. The threshold of about 2.5 ± 0.4 eV (4.9 ± 0.8 eV lab) suggests the possibility that there was a small O_2 contaminant, which reacts with Co^+ to form CoO^+ with a threshold at a laboratory energy of 5.06 ± 0.14 eV.[34]

(34) Fisher, E. R.; Elkind, J. L.; Clemmer, D. E.; Georgiadis, R.; Loh, S. K.; Aristov, N.; Sunderlin, L. S.; Armentrout, P. B. *J. Chem. Phys.* **1990**, *93*, 2676.

(35) Armentrout, P. B. *ACS Symp. Ser.* **1992**, *502*, 194.

(36) Taylor, J. R. *An Introduction to Error Analysis*; University Science Books: Mill Valley, CA, 1982.

(37) Jackson, T. C.; Carlin, T. J.; Freiser, B. S. *Int. J. Mass Spectrom. Ion Processes* **1986**, *72*, 169.

(38) McMahon, T. J.; Jackson, T. C.; Freiser, B. S. *J. Am. Chem. Soc.* **1989**, *111*, 421.

(39) Loh, S. K.; Fisher, E. R.; Lian, L.; Schultz, R. H.; Armentrout, P. B. *J. Phys. Chem.* **1989**, *93*, 3159.

(40) Armentrout, P. B.; Kickel, B. L. In *Organometallic Ion Chemistry*; Freiser, B. S. Ed.; Kluwer Academic: Dordrecht, 1996; p 28.

(41) Fisher, E. R.; Armentrout, P. B. *J. Phys. Chem.* **1990**, *94*, 1674.

(42) Fiedler, A.; Hrušák, J.; Koch, W.; Schwarz, H. *Chem. Phys. Lett.* **1993**, *211*, 242.

(43) Fiedler, A.; Schröder, D.; Shaik, S.; Schwarz, H. *J. Am. Chem. Soc.* **1994**, *116*, 10734.

(44) (a) Schröder, D.; Schwarz, H.; Shaik, S. *Struct. Bonding*; Springer-Verlag, Heidelberg, **2000**, *97*, 91. (b) Kretzschmar, I.; Schröder, D.; Schwarz, H.; Armentrout, P. B. In Advances in Metal and Semiconductor Clusters; Duncan, M. A., Ed.; **2001**, *5*, 347.

(45) Schultz, R. H.; Crellin, K.; Armentrout, P. B. *J. Am. Chem. Soc.* **1991**, *113*, 8590.

(46) Tjelta, B. L.; Armentrout, P. B. *J. Phys. Chem. A* **1997**, *101*, 2064.

(47) Goebel, S.; Haynes, C. L.; Khan, F. A.; Armentrout, P. B. *J. Am. Chem. Soc.* **1995**, *117*, 6994.

(48) Barnes, L. A.; Rosi, M.; Bauschlicher, C. W. *J. Chem. Phys.* **1990**, *93*, 609.

(49) The collision cross section is predicted using the Langevin−Gioumousis−Stevenson (LGS) model (ref 50), $\sigma(\mathrm{LGS}) = \pi e(2\alpha/E)^{1/2}$ where α is the polarizability of the neutral reactant (5.71 $Å^3$ for COS, ref 51) and E is the relative kinetic energy of the reactants.

(50) Gioumousis, G.; Stevenson, D. P. *J. Chem. Phys.* **1958**, *29*, 292.

(51) Miller, K. J. *J. Am. Chem. Soc.* **1990**, *112*, 8553.